Communications In Catalysis
Vol. 1, No. 2, 2018, pp.1-12
DOI: 10.22049/CIC.2018.26191.1019

Azarbaijan Shahid Madani University

The Effect of Pt Thin Films on Efficiency of the Carbon-Based Catalysts for Proton-Exchange Membrane Fuel Cells

Shahab Khameneh Asl[a*], Saeed Behjat[a]

[a]Materials Eng. Department, Mechanical Eng. Faculty, University of Tabriz, Tabriz, IRAN, P.O. Box 5166614766

Corresponding Author. Tel: +9841333922468, Fax: 984133377866
E-mail: address:shah.kh.asl@gmail.com,
Received: 2018-04-25, Revised: 2018-06-19, Accepted:2018-07-01

Abstract

With increasing pollution and decrease in global reservoirs of fossil fuels, a lot of interest has been attracted to fuel cells as efficient and clean energy sources. Polymeric (membrane) fuel cells are special type of fuel cells, which can be built in small dimensions and power. These cells use hydrogen (and oxygen or air) and produce water. In these cells, platinum is used as electrode (and electro catalyst) both in anode and cathode, due to its low overvoltage for both hydrogen and oxygen. To increase the efficiency of these coatings, it is best to produce platinum particles with maximum area and it automatically leads to nanometric particles. In this thesis, platinum particles are electrodeposited first on Floride doped Tin Oxide (FTO) and then on graphite. Electro deposition is conducted via DC and pulse methods. Floride doped Tin Oxide (FTO) samples have been examined using voltametry in 0.5M H_2SO_4 and graphite samples have been examined in 0.5 M H_2SO_4 + 0.5 M CH_3OH. Specific area of platinum on Floride doped Tin Oxide (FTO) substrates has been calculated. In graphite substrates, comparative analysis has been performed. Prepared samples have been examined using scanning electron microscope. For Floride doped Tin Oxide (FTO) sample, AFM test has been performed to approve the results of SEM. According to results, Platinum particles with approximate diameter of 30 nanometers have been successfully coated on Floride doped Tin Oxide (FTO) and graphite.

Keywords: Nanometric coating, Pulse Electro deposition, Pt/C, Polymeric fuel cells

Introduction

Sir William Grove was the first to build a real fuel cell in 1839 after succeeding in constructing a larger battery (Pew Groove) in 1838. Fuel cells are less polluting than traditional heavy-duty batteries with toxic materials and hazardous nuclear technology. Unlike internal combustion engines that burn fossil fuels and produce toxic gases, the use of fuel cells is the only final product of water vapor [2]. Fuel cells are divided according to the type of electrolyte and type of electrode. Typically, this category includes four major groups. Solid oxide cells, alkaline molten salt cells, sulfuric acid powders and polymer powders. Polymer cells work at ambient temperature and use conductive polymers as electrodes. These fuel cells have been created from a solid polymer electrolyte with porous channels to facilitate the transfer of ions. Due to practical problems with the use of liquid electrolytes, porous or penetrating solid membranes are used in PEM fuel cells [2].

The governing equations for these cells are as follows:

(1) anode $2H_2 \xrightarrow{yields} 4H^+ + 4e^-$

(2) cathode

$$O_2 + 4H^+ + 4e^- \xrightarrow{yields} 2H_2O$$

(3) total reaction

$$2H_2 + O_2 \xrightarrow{yields} 2H_2O\ E^0 = 1.23\ V$$

The theoretical potential of the fuel cell reaction shown above is calculated as follows, which is equal to 1.23 V

(4) $$E^0_{theoretical} = -\frac{\Delta G^0}{nF}$$

During the operation of a fuel cell in non-standard conditions, the activity of the reactants and products is not equal to one, therefore, the voltage of the cell should be calculated from the relation Nernst:

(5) $$E_{theoretical} = E^0_{theoretical} + \frac{RT}{nF} ln \left[\frac{(p_{H_2})(p_{O_2})^{1/2}}{p_{H_2O}}\right]$$

$E_{theoretical}$ is Theoretical voltage of the cell in non-standard conditions, $E_{theoretical}^0$ is Theoretical voltage of the cell under standard conditions, P_{H2}, P_{O2}, and P_{H2O} are the partial pressures of hydrogen, oxygen and water, F Faraday's constant (96485 col / mol), n is the number of electrons produced per mol of hydrogen consumed, R is the global gas constant and T is Kelvin's temperature. By increasing the partial pressure (or concentration) of the reactants, the $E_{theoretical}$ column can be increased [3]. In fact, the actual voltage is lower than the theoretical voltage. Because of the low voltage of oxygen and hydrogen on platinum, these drops are minimized for platinum [4]. so, in polymer platinum systems, platinum acts as a catalyst. Platinum covers, however, have many applications in other catalysts, too [5].

The first experiments on platinum electrolyte deposition, conducted more than 150 years ago by Ellington, who in 1837 recorded a patent certificate in his name, was later followed up by the investigator [6]. In general, today's electrolytes, containing platinum, are stable and very complex. An advantage of these complexes is that they exhibit fewer tendencies to hydrolysis in the bath than

simple salts, and thus the electrolytes are more stable [6]. These electrolytes can be divided into two groups, platinum-containing baths in bivalent and quadrupole states, can be further differentiated in each case with regard to the salts used, which are not always the same as those of the metal sources. In this context, a variety of platinum deposition methods from the chloroplatinic acid solution can be referred to as a deposit at the constant potential of the constant potential deposition (CPD). In a CPD, a potential is applied to the cathode in which platinum (or any other metal) can precipitate until Metallic ions close to the surface. Particle growth is controlled by changing the solution concentration, potential, ionic strength, pH or sedimentation time and electrode [5]. In the PED electrochemical pulsed sedimentation method, negative potential is applied in small time intervals and precipitates the metal from a solution containing ion. In Pulse electrodeposition (PED), a continuous pulse repeats with a light pulse that goes off with a silent pulse, but with an opposite load (or a differential potential other than the potential that the metal precipitate). In addition, platinum nanometer coatings have numerous and growing applications in various industries. Platinum coatings have been applied in different ways on different substrates. Zelenovich, Tripkovich and Rafilevich have covered platinum by thermal decomposition on titanium and examined the methanal oxidation [7]. To do this, the titanium surface has been shaken first to improve adhesion and better bonding. In another study, by Ziao, Blanar and Manoharan, the effect of platinum coverage on zirconia in oxygen sensors has been investigated [8]. In a research conducted by Sallikova, electrochemical sedimentation of platinum from a chlorinated molten bath has been investigated [9]. In another interesting study, Lee, Chan and Phillips have studied the growth of two-dimensional and three-dimensional dendrites in platinum nanoparticles of electrical deposition. As previously mentioned in the same section, platinum tends to produce two-dimensional dendrites in the direction of 110 and three in the direction of 100 [9]. However, this issue has been observed in smaller dimensions. In another study, Driff, Walter and Penn, have deposited particles and platinum nano wires using a galvanic displacement on the Highly Ordered Pyrolytic Graphite (HOPG) substrate [10]. In another research by Huang and Tsai, the electroplating of platinum nanoparticles in carbon-naphtha nanocomposites has been investigated. The purpose of this coating was catalytic properties in the oxidation of methanol [11]. In the older work, Zubimindy, Vasquez, Echo, Vara, Triassic, Sallaraza and Arroyo, the early stages of the platinum sedimentation have been investigated on HOPG [12]. In this paper, there are two goals to be considered: an examination of the effective parameters in increasing the efficiency of the catalysts used in the fuel cells by reducing the grain size and optimizing the conditions in such a way that these factors can be controlled. The ultimate goal of this study is to reduce the particle size of the platinum and increase the fuel cell efficiency. To do this, with regard to what was said, it tried to cover the platinum from its ion-containing solution (chloroplatinic acid H_2PtCl_6) by pulse method. To optimize the conditions, a commercially-operated, electrically controlled system was used.

Experimental procedure

Sedimentation was performed on the FTO glass slabs (Pilkington TEC 15 / 3.2 produced by KINTEC) and graphite (SK1, Seraj Industrial Coal).

Chloroplatinic acid solution was used to precipitate the platinum tetrachloride to prepare it. Potassium tetrachloride (Fluka Chemicals, 100% pure, containing 58% platinum), powdered by adding a stoichiometric amount of concentrated chloride (Merck Chemicals, containing 37.5% HCl in 100 g of solution) and deionised water, dissolves 40 mM of chloroplatinic acid as the base solution was prepared. To control pH from concentrated sulfuric acid (Merck Chemicals, 95-97% H_2SO_4 in 100 g of solution). To prepare the samples for coating, the base with deionized water and ethanol was placed in the ultrasonic cleaner.

In order to apply the constant potential coatings, the Princeton Appliediscount Princeton Opportunity R & C Preston potentiostat / galvanostat EG & G model 273A as well as the Autolab Potentiostatic / Galvanostat PGSTAT 302N was used. Four pulsed samples were prepared according to Table 1 (two FTO samples and two graphite samples) assigned to P1 and P2, and GP1 and GP2. These four samples were precipitated from 0.01 M chloroplatinic acid solution. P1 and GP1 samples were prepared at a pulse voltage of ± 1000 mV (saturated calomel electrode:SCE) and samples of P2 and GP2 at a pulse voltage of ± 500 mV (SCE).

In order to investigate FTO samples, cyclic voltammetric test was used. In these tests, the Autolab device PGSTAT 302N was used in the corrosion lab of Sharif University of Technology. To investigate the surface microstructure of the coating, an ordinary scanning electron microscope of the Razi metallurgy research center and a scanning electron microscope of the Electrical Department of the Faculty of Engineering of the University of Tehran using the HITACHI S4160 model were used. For comparison of SEM images, for example, the FTO was used for atomic force microscopy. The atomic force microscope was used by the associate professor, the Nanosurf model of the Mobile S model.

The metal distribution on the surface of the samples was measured by a system designed to measure the isotherm of hydrogen adsorption. After resuscitation of samples using hydrogen atmosphere at 350 °C, the coating was cooled under vacuum conditions and the isotherm was poorly absorbed and the total pressure was measured at 1-40 rounds at room temperature. The difference between poor absorption and total up to zero pressure was achieved. This indicates a strong absorption of hydrogen, which is generally absorbed on the coating surface metals, now assuming a ratio of one to one hydrogen atom and metal (platinum), the amount of metal surface was measured [13].The heat of absorption of catalyst samples was obtained by using a calorimeter attached to a glass compartment of a C-80 tian-Calvet calorimeter vacuum tube equipped with a diaphragm pump turbomolecule. For measuring the pressure with a Varian CeramiCel pressure gauge in a range of 10 to 10, the negative power of four rounds was used.

Table 1. Specifications of samples and their codes

Sample code	Substrate	Type	Test conditions	analysis	Surface (cm^2)
P1	FTO	Pulse precipitation	Cubic pulse ±1000mV (SCE)	FESEM, cyclic voltammetry 0.5 M H_2SO_4	1.2579
P2	FTO	Pulse precipitation	Cubic pulse ±500mV (SCE)	FESEM, cyclic voltammetry 0.5 M H_2SO_4AFM	1.1855
GP1	Graphite	Pulse precipitation	Cubic pulse ±1000mV (SCE)	FESEM, cyclic voltammetry 0.5 M H_2SO_4, 0.5 M CH_3OH	1.6393
GP2	Graphite	Pulse precipitation	Cubic pulse ±500mV (SCE)	FESEM, cyclic voltammetry 0.5 M H_2SO_4, 0.5 M CH_3OH	0.9577

Results and discussions

The potentials are more positive than the equilibrium potential (Nernistis) [14]. This state usually occurs at the level of an atomic layer, and very rarely of two layers, and in the case of hydrogen on platinum, Underpotential deposition (UPD) can be considered as one layer at high approximation. Each atom of platinum on the particle surface (each surface atom) has the ability to absorb a hydrogen atom. The shape, size, and number of peaks observed on the hydrogen absorbed in a CV depend on the crystalline arrangement of the particle platinum [15]. In addition, the intensity and shape of the absorption and discharging peaks of hydrogen depend on the purity of the electrode, the solubility of the impurities and the nature of the electrolyte. However, the voltage and position of the UPD-related couriers, with a very good approximation, are independent of the speed of the scan and the switching voltage [14]. The area below the UPD Chart is a measure of the load exchanged during the absorption of hydrogen. This time, it specifies the number of hydrogen atoms that are absorbed during the process on the surface of platinum atoms. Given that each atom of platinum absorbs only one hydrogen atom, the number of platinum atoms can be obtained at the electrode surface. In the case of samples with a high background signal of hydrogen and comparable to platinum itself, it is not possible to check the level of platinum with hydrogen UPD. The FTO does not actually produce a signal that is problematic, but carbon intensely raises the signal and will probably hide the UPD-related signals from hydrogen. In this case, other methods are used to check the level of platinum. A methanol solution with half a molar sulfuric acid can be used and methanol oxidation on platinum is studied. With these issues in mind, for the qualitative analysis of (Cyclic Voltammetry) CVs obtained for graphite samples, it can be said that the higher the level below the charts of these peaks (at a scanning speed), the greater

the amount of platinum on the surface. Due to the broader and longer methanol oxidation, this peak was used for data analysis [16,17].

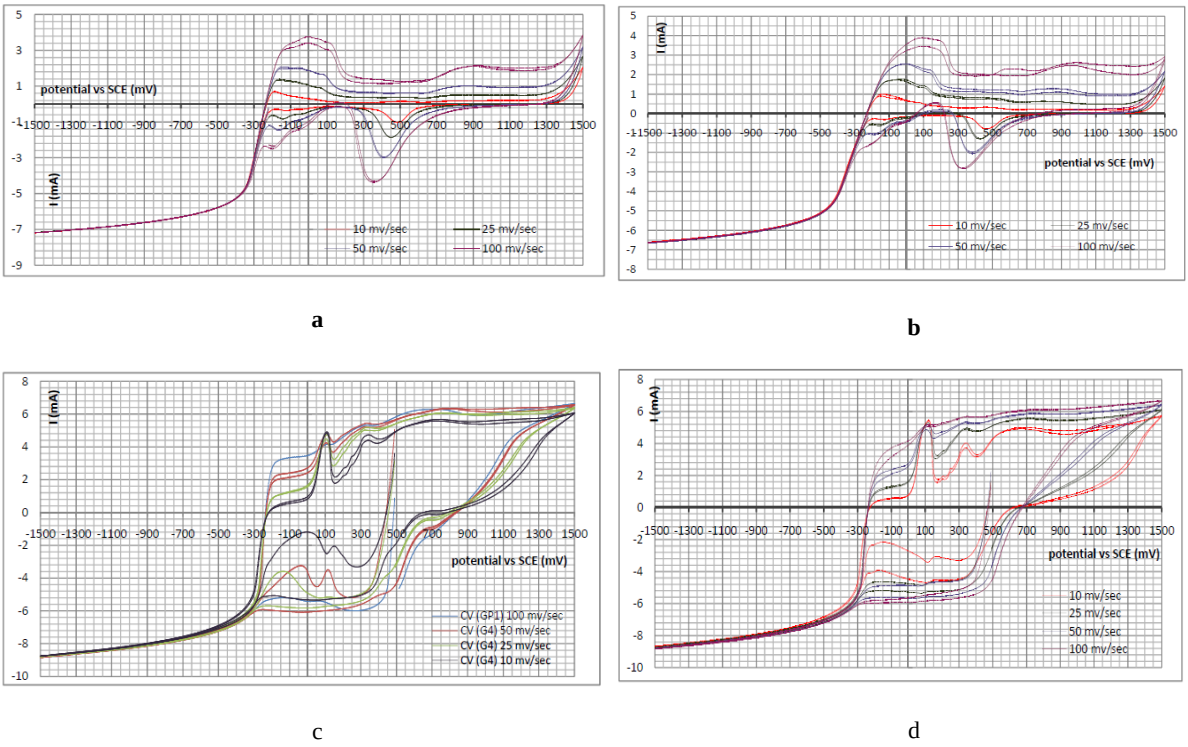

Figure 1. The cyclic voltammetry (CV) of the samples P1 (A) and P2 (B) in a 0.5 M H_2SO_4 solution is two cycles and refers to GP1 (C) GP2 (d) in a solution of + CH_3OH 0.5 M H_2SO_4 0.5 M.

Figure 1 (a) shows the results of the cyclic voltammetric sample P1 (FTO substrate, produced in a pulse of ± 1000 mV (SCE)) in a single cycle at four different scan speeds. The electrode is Ag / AgCl. This test was performed at a reference electrode voltage of SCE = +0.149 mv, the scanning speed was mv / sec 100; the first switch point was 1500 mv (SCE); the second switch point was 1500+ mv (SCE). The surface area of platinum in this sample was calculated as 1.2579 square meters. In Fig. 1b, the results of the cyclic voltammetric of the sample P2 (FTO substrate, produced in a pulse of ± 500 mV (SCE)) in two cycles and at four different scan speeds, respectively, showed a platinum surface area of 1855.1 m^2 Calculated. In the voltammetric studies of graphite specimens, as already mentioned, Hupd's analysis of graphite is not accurate due to the high signal. In this case, methanol oxidation was used. Due to the fact that quantitative analysis by methanol oxidation was not mentioned in the sources, the qualitative analysis of CVs obtained for graphite specimens was determined. In general, it can be said that the higher the level below the charts of these peaks (at a scan speed), the greater the amount of platinum on the surface. Here, too, graphs have been used to show the methane's main courier. Due to the lack of oxygen removal, the resulting charts also have oxygen peaks, which make their analysis a bit more complicated.

Fig. 1C shows the results of the cyclic voltammetric sample GP1 (graphite

substrate, prepared in a pulse of ± 1000 mV (SCE)) in a cycle at four different scan speeds. The platinum level in this sample was 6,393 square meters, which is comparable to that of the FTO. Also in Fig. 1d, the cyclic voltammetric results show the GP2 sample (graphite substrate (SCE)) in a four-speed scan. The platinum level of this sample was 9.577 m^2, which has a noticeable drop in comparison with other samples.

SEM images were prepared from the surface of prepared samples for microstructure analysis of coated samples. Figure 2 (a) to (b) related to the sample P1. In this sample, a portion of the coating was dug during the deposition (it was torn off from the surface), however, until the end of the desired cycles, the test was performed. This image (2) is related to that area. In the area covered, the effects of platinum remained that had branches in the branch. The darker background is the FTO. The magnification of this image is 800 times, after the growth of the platinum layer was grown in layered regions where the platinum structure in that area, as it is seen, was a branch of the branch. This dendrite growth state, as previously mentioned, is common in platinum [9,18,19]. But so far, no pulsed precipitation has been reported.

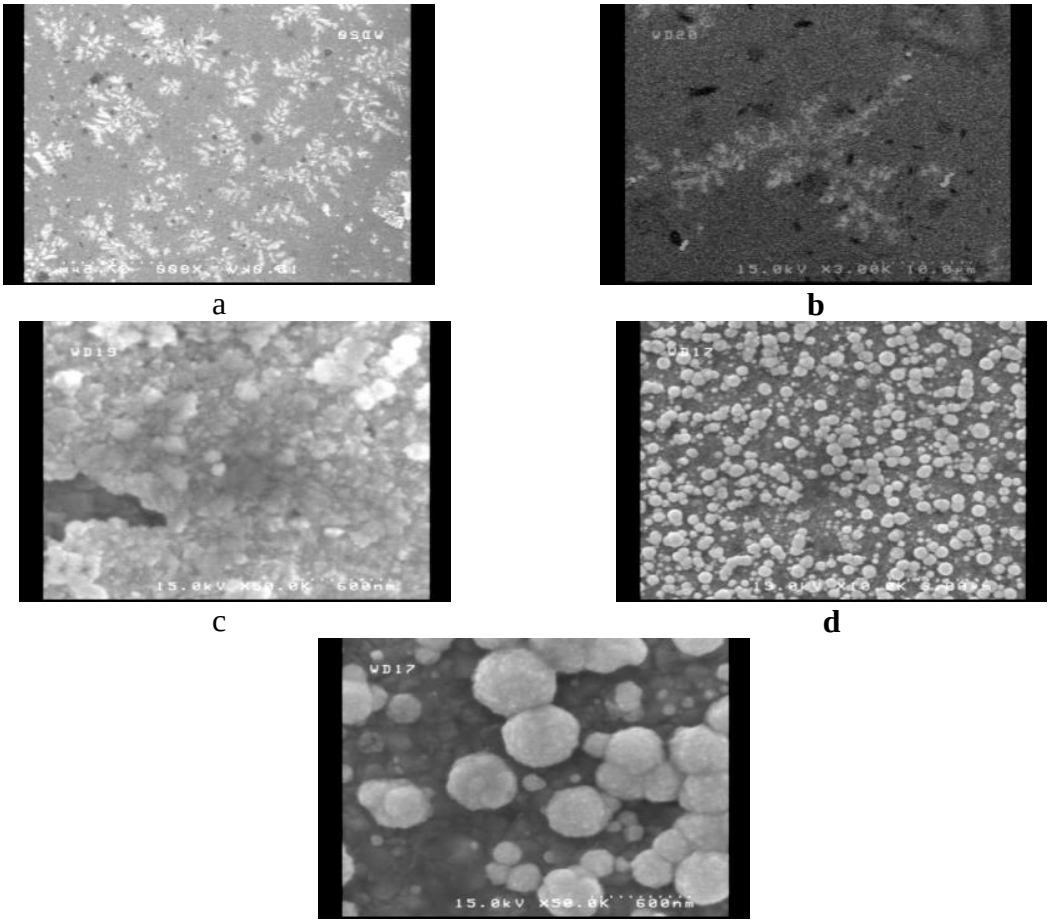

Figure 2. Image of Field Emmition Scanning Electron Microscopy (FESEM) from sample P1. Zoom 800 times (A), 3000 x (B), 50000 x (C), from sample P2. Magnification 15000 x (d), 50,000 x (e).

In Figure 2B, one of these branches is larger and is magnified 3,000 times, which is evident in the development of dendritic form. At this stage, growth is two-dimensional. In Fig. 2C, the sample surface in an apparently unplanned area shows a magnification of 50,000 times. The platinum layer has been completed and agglomerated on a platinum complete layer. However, a hole in this area can be seen without difficulty showing the surface of the FTO. The fine white particles are platinum, which is about 20 nm in size, and the dark field is FTO. The darkness in the middle of the image is due to the accumulation of electron microscopic load.

Figure 2d, e, refers to the sample P2. In this image, taken at a magnification of 10,000 times, the fine and coarse particles of platinum, all of which are spherical, are well visible. The sedimentation voltage of this pulsed sample is lower and the platinum layer does not cover the full FTO surface. In Figure 2, the part marked in the previous figure is displayed at a magnification of 50,000 times. Extremely fine particles of platinum and two relatively large particles, all of which are spherical, are visible. Particles have different sizes and apparently at the growth stage. The surface of this sample was excellent, but unclear and dark. You can see the dimensions of these particles in this shape. In this image, platinum particles are visible from 56 to 344 nm. With greater magnification, the surface of the particles of platinum is visible. The surface of each particle consists of infinitely many fine particles of platinum, each of which is single. According to these images, it is clear that in samples P, the coating contains platinum nanoparticles. However, the goal of this project is to apply coating on graphite, and success at this stage is not enough.

For GP1, the first image, Figure 3a, is magnified by 1000 times. In the image of the graphite surface, where particles of platinum are not recognizable on its surface, some areas are unevenly visible. Expecting to see nanometric particles in this magnification is futile. However, due to the unspecified, a white streak is seen in the middle of the image.

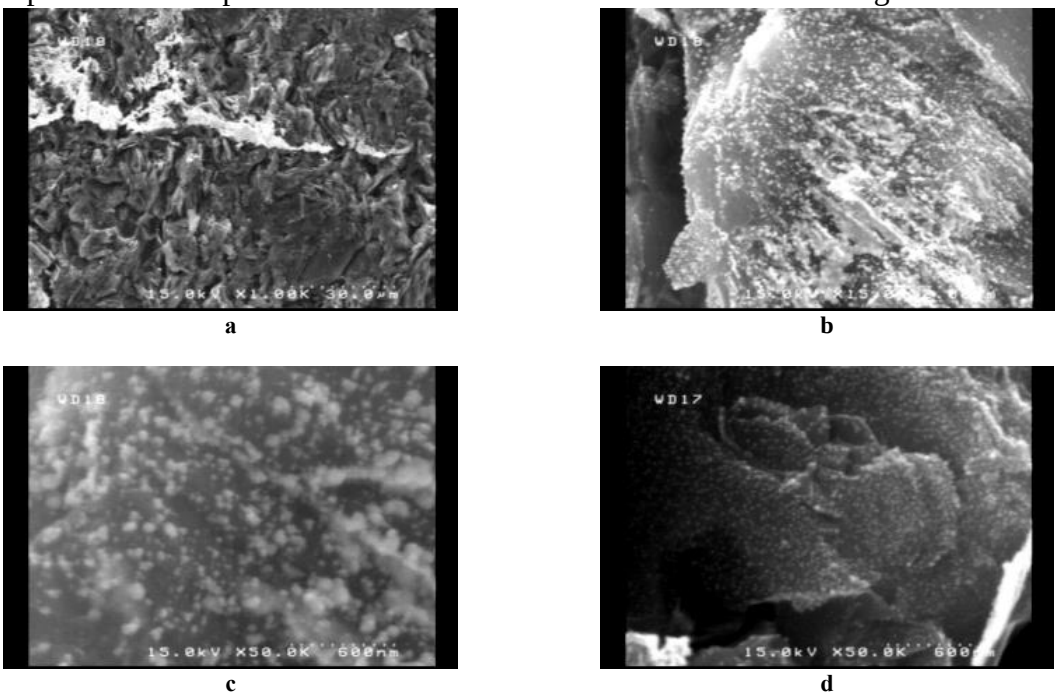

a **b** **c** **d**

Figure. 3. Figure of the field emission scanning electron microscope (FESEM) from the GP1 specimen. Zoom 1000 x (A), 15000 x (B), 50,000x(C) of GP2 sample. Magnification is 50,000 x (d).

In Figure 3b, which is shown with a magnification of 15,000 times, the surface of graphite deposited on the platinum particles is well known, although the more interlayer surfaces are graphite without deposition, single platinum particles are definitely on its surface. In the middle areas of the image (where it is marked with red circles), fine particles are mixed together and coarse particles are created. Agglomeration is also observed in areas. At a magnification of 50,000 times the image of 3C, platinum particles are still tiny. Despite the conductivity of graphite, the accumulation of load in this sample was very severe and allowed to go to higher magnifications hardly. That's why the image is blurry. In Fig. 3C, too many platinum particles are cut. Particle sizes in this sample are estimated at a maximum of 30 nm. Also, Figure 3d shows the image of the field emission scanning electron microscope (FESEM) from the GP2 specimen. The magnitude of the 50,000-fold increase shows the island's growth of platinum particles (in the range of several nanometers in the range of 10 to 20 nanometers) in this image, although the lower density of these particles indicates a limited sedimentation rate for these particles. The result with the platinum level calculations, cyclic curves can also be verified.

The FTO sample of the atomic microscope was also used to confirm the SEM data. AFM images were obtained from the samples, which was not possible due to the porous graphite structure. This was done for the P2 sample. Two images were prepared for the P2 sample, one in the size of 4 μ m × 4 μ m and another 2 μ m × 2 μ m. Using AFM, in addition to topography, fuzzy properties can also be determined, because the different genus of the atom under the probe causes the input signal to vary. Platinum The bulges seen in the brighter topographic image correspond to the prominences in the fuzzy image, which represent particles of platinum. Given that the platinum cover is pure, and according to SEM images, expect this behavior to be logical. Meanwhile, these areas have a circular cross section. At the bottom of the image, the particles of platinum are clearly visible alongside. Now, these regions with circle cross-section (spheres) have different fuzzy contrast, that is, they have different sexes. These are the same particles of platinum.

In Figure 4 a and b, the topographic and fuzzy signals are compared. The bulges seen in the brighter topographic image correspond to the prominences in the fuzzy image, which represent particles of platinum. Given that the platinum cover is pure, and according to SEM images, expect this behavior to be logical. Meanwhile, these areas have a circular cross section. At the bottom of the image, the particles of platinum are clearly visible alongside. Now, these regions with circle cross-section (spheres) have different fuzzy contrast, that is, they have different sexes. These are the same particles of platinum. In the fuzzy image due to the fuzzy contrast, small particles of platinum also appear in the topographic image of the valleys.

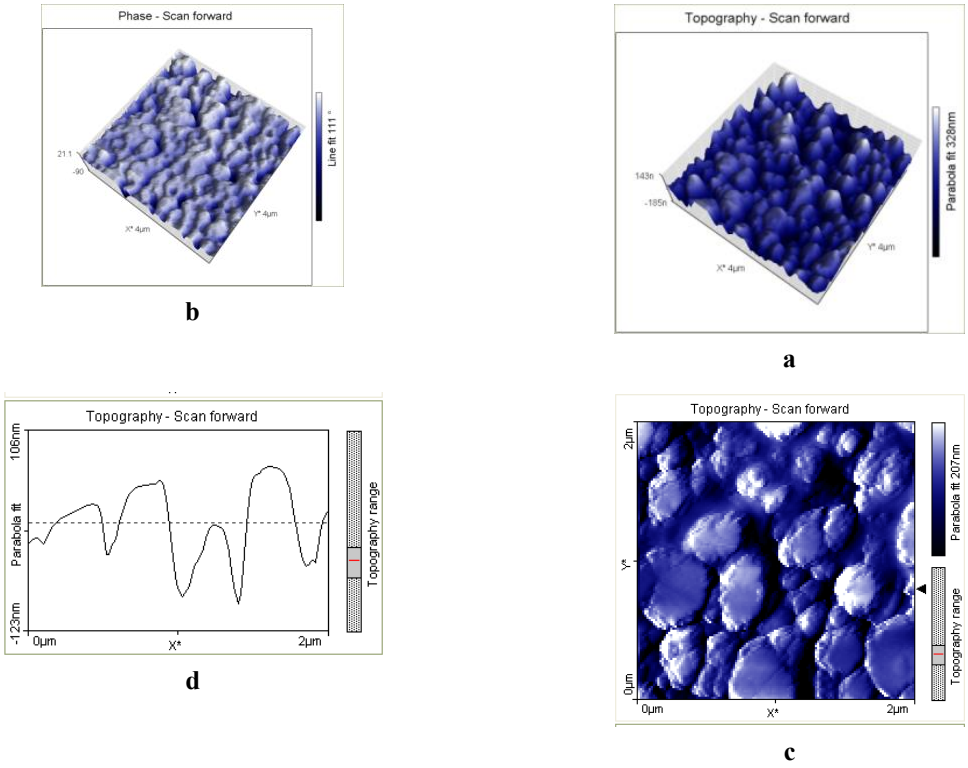

Figure 4. The atomic force microscope image (AFM) of sample P2. The dimensions of the image are 4 μ m × 4 μ m, the height dimension is also displayed in this 3D image; here the fuzzy image (A) and the topographic image (B) of the image are 2 μ m × 2 μ m, in the topography (C), the height profile of the drawing (D)

The image of 4C is four times larger than the previous one and is also here adapted. Given this shape, it cannot be said that the particles are definitely spherical. They may be disc shaped. The height profiles in Fig. 4d shows, according to the profile, the particle height changes gradually and slightly on each single particle. According to this picture, the probability of spherical particles is greater than their disks. In this image, the size of a large particle is 303 nm. This result is consistent with the SEM images for the P2 sample.

The distribution of platinum in various coating surfaces using isotherms and the absorption heat associated with the presence of platinum in the coating is summarized in Table 2. [The results show that the GP1 specimen has a higher heat and coating surface that can be compared and verified according to the results of cyclic voltammetry and electron microscopic images.

Table 2. Type of coatings and Pt Concentration, %coverage and H_2adsorption energy

Sample name	% coverage	Heat od adsorption (Kj/mol)
P2	16.6	**92**
GP2	9.8	**86**
P1	12.1	**89**
GP1	26.9	**93**

Conclusions

According to the results, it can be concluded that optimal cyclic platinum conditions were found on FTO and graphite glass. The results of microscopy and voltammetric data and isotherms show the stability of absorption and the amount of platinum in the synthesized samples in accordance with the working conditions. Graphitic specimen GP1 provides the highest sediment rate and the highest level of platinum, which is very suitable for the use of fuel cell electrode. Also, the platinum sediment morphology was spherical in all cases. In cases where the growth rate was high, growth was rapidly converted to three-dimensional growth, and eventually caused the platinum layer to separate from the substrate. This was associated with platinum agglomeration. The platinum sediment on the FTO does not have much stability and is easily detached. In the case of pulsed samples on graphite, the surface layer stability was higher.

References

[1] Srinivasan. S, Mosdale. R, Stevens. P and Yang. C, Ann. Re. of Energ. Environ., 1999, 20.

[2] Mateo. J. J, Tryk. D. A, Cabrera. C. R and Ishikawa. Y, Mol. Simul., 2008, 34, 1065,10-15.

[3] EG&G Tech. Serv. Inc., in Fuel Cell Handbook, U.S. DOE. Office of Foss. Energ. Nati. Energ. Tech. Lab, 2005, 15-45.

[4] Larminie. J and Dicks. A, in Fuel Cell Sys. Explaind, 2nd ed., Chichester, JW, 2003, 67-119.

[5] Hoogers. G, in Fuel Cell Tech. Handbook, CRC, 2003, 137-160.

[6] Hideya Okamoto, President & CEO , Tanaka Holdings Co.,Ltd, 2010.

[7] Baumgarner. M. E and Raub. C. J, Platin. met. Rev., 1988, 32. 4, 188.

[8] Zelenovic-Ribic. L, Tripkovic. A and Rafailovic. L, Acta Agric. Serb,2005, 19. 33.

[9] Xiao. H, Blanar. T and Manoharan. R, Rosemount Analytic. Inc. Orrville, OH, 2010, 44667.

[10] Saltykova. N. A, JOM, 2003 , 201, 39. 1-2.

[11] Dryfe. R. A. W, Walter. E. C and Penner. R. M, Europ. J. Phys. Chem, 2004, 5,1879.

[12] Hong. Y. H and Tsai. Y. C, J. Nanomater, online edition, 2009, 1.

[13] Zubeimendi. J. L, Vazquez. L, Ocon. P, Vara. J. M, Triaca. W. E, Salvarezza. R. C and Arvia. A. J, J. Phys. Chem, 1993, 97, 5095.

[14] Anpo. M, Kamat. P, Uner. D, Book Chapter of environ. design cat., Springer, Germany, 2009.

[15] Flores Araujo. S. C, Electrochemical Study of Under-Potential Deposition Processes On Transition Metal Surfaces, Austin: University of Texas, 2006.

[16] Mateo. J. J, Tryk. D. A, Cabrera. C. R and Ishikawa. Y, Mol. Simulat, 2008 , 1065, 34. 10-15.

[17] Stevanović. S, Tripković. D, Kowal. A, Minić. D, Jovanović. V. M, Tripković. A, J. Serb. Chem. Soc. 2008 73, 845,8–9.

[18] Tripkovic. A. V, Gojkovic. S. Popovic. L. K. D and Lovic. J. D, J. Serb. Chem. Socy, 2006, 71. 12,1333.

[19] Lee. I. S, Chan. K. Y and Philips. D. L, JJAP, 2004, 43, 767.
[20] Hill. A C, Patterson. R, Sefton. J. P and Columbia. M. R, "NLM, 1999, 15, 11, 4005.